PROCEEDINGS OF SCIENCE

Semileptonic decays of K and D mesons in $2+1$ flavor QCD

Jon A. Bailey[a] A. Bazavov[b], C. Bernard[c], C. Bouchard[d], C. DeTar[e], A.X. El-Khadra[d], E.D. Freeland[c], E. Gámiz*[a], Steven Gottlieb[f,g], U.M. Heller[h], J.E. Hetrick[i], A.S. Kronfeld[a], J. Laiho[j], L. Levkova[d], P.B. Mackenzie[a], M.B. Oktay[d], J.N. Simone[a], R. Sugar[k], D. Toussaint[b], and R.S. Van de Water[l]

[a] *Fermi National Accelerator Laboratory, Batavia, IL 60510, USA*
[b] *Department of Physics, University of Arizona, Tucson, AZ 85721, USA*
[c] *Department of Physics, Washington University, St. Louis, MO 63130, USA*
[d] *Physics Department, University of Illinois, Urbana, IL 61801, USA*
[e] *Physics Department, University of Utah, Salt Lake City, UT 84112, USA*
[f] *Department of Physics, Indiana University, Bloomington, IN 47405, USA*
[g] *National Center for Supercomputing Applications, University of Illinois, Urbana, IL 61801, USA*
[h] *American Physical Society, One Research Road, Ridge, NY 11961, USA*
[i] *Physics Department, University of the Pacific, Stockton, CA 95211, USA*
[j] *SUPA, School of Physics & Astronomy, University of Glasgow, Glasgow, G12 8QQ, UK*
[k] *Department of Physics, University of California, Santa Barbara, CA 93106, USA*
[l] *Department of Physics, Brookhaven National Laboratory, Upton, NY 11973, USA*

Email: egamiz@fnal.gov

Fermilab Lattice and MILC Collaborations

The experimentally measured rates of the semileptonic decays $K \to \pi l \nu$ and $D \to K(\pi) l \nu$ can be combined with lattice calculations of the associated form factors to precisely extract the CKM matrix elements $|V_{us}|$ and $|V_{cs(d)}|$. We report on the status of form factor calculations with Fermilab charm quarks and staggered light quarks on the 2+1 flavor asqtad staggered MILC ensembles. Analysis of data for the $D \to \pi l \nu$ form factor provides a nontrivial test of our methods via comparison with CLEO data. We discuss the use of HISQ valence quarks to calculate the $K \to \pi l \nu$ form factor $f_+^{K\pi}(0)$ and describe tests of our method.

The XXVIII International Symposium on Lattice Field Theory, Lattice2010
June 14-19, 2010
Villasimius, Italy

*Speaker.

PoS(Lattice 2010)306

1. Introduction

Studies of exclusive semileptonic decays of B, D, and K mesons are used to extract the Cabibbo-Kobayashi-Maskawa (CKM) matrix elements $|V_{ub}|$, $|V_{cb}|$, $|V_{cs}|$, $|V_{cd}|$, and $|V_{us}|$ with errors competitive with those obtained using inclusive semileptonic decays, leptonic decays, neutrino-antineutrino interactions, and τ decays [1]. The theory inputs needed to fix the CKM matrix elements from exclusive semileptonic widths are form factors parameterizing corresponding hadronic matrix elements:

$$\langle P_2|V^\mu|P_1\rangle = f_+^{P_1P_2}(q^2)(p_{P_1}+p_{P_2}-\Delta)^\mu + f_0^{P_1P_2}(q^2)\Delta^\mu\,, \tag{1.1}$$

where $\Delta^\mu = (m_{P_1}^2 - m_{P_2}^2)q^\mu/q^2$, $q = p_{P_1} - p_{P_2}$, and V is the appropriate flavor-changing vector current. Alternatively we may write [2]

$$\langle P_2|V_\mu|P_1\rangle = \sqrt{2m_{P_1}}[v_\mu f_\parallel^{P_1P_2}(q^2) + p_{\perp\mu} f_\perp^{P_1P_2}(q^2)], \tag{1.2}$$

where $v = p_{P_1}/m_{P_1}$ and $p_\perp = p_{P_2} - (v\cdot p_{P_2})v$, so that in the rest frame of a heavy meson P_1,

$$f_\parallel^{P_1P_2}(q^2) = \frac{\langle P_2|V^0|P_1\rangle}{\sqrt{2m_{P_1}}} \quad \text{and} \quad f_\perp^{P_1P_2}(q^2) = \frac{\langle P_2|V^i|P_1\rangle}{\sqrt{2m_{P_1}}}\frac{1}{p^i_{P_2}}. \tag{1.3}$$

Typically, theoretical errors in the form factors limit the accuracy of such extractions of the CKM matrix elements. The situation has been acute in the case of D semileptonic decays [3]. Here we describe calculations of D and K semileptonic form factors, which provide access to $|V_{cs(d)}|$ and $|V_{us}|$, respectively.

For D decays we seek not only the CKM matrix elements, but also to validate applying our methods to the B decays $B\to\pi l\nu$ and $B\to Kl\bar{l}$. Below we use a subset of the available lattice data to check our methods; we compare the shape of a preliminary result for the $D\to\pi l\nu$ form factor with the shape as measured by CLEO [3]. For D decays, unlike B decays, the lattice and experimental data overlap throughout most of the q^2 domain, affording a more powerful check.

Precise determinations of $|V_{us}|$ provide stringent tests of first-row unitarity and may furnish additional information about the scale of new physics [4]. Here we describe the main ingredients of our strategy to use staggered quarks to obtain $f_+^{K\pi}(0)$ and the tests we have performed to verify that our approach will yield errors competitive with existing calculations of the form factor.

2. $D\to\pi l\nu$: Extraction of $|V_{cd}|$

2.1 Ensembles and valence masses

We have completed generating correlators with Fermilab heavy quarks and asqtad staggered light quarks on the 2+1 flavor asqtad staggered MILC ensembles shown in Table 1. The heavy quark is tuned to the charm mass on each ensemble, and the light valence masses include partially quenched and full QCD points. In addition to the ensembles shown in Table 1, we are generating correlators on a fine ensemble with $m_l = 0.15m_s$, superfine ensembles with $m_l \approx 0.14m_s,\ 0.1m_s$, and an ultrafine ($a\approx 0.045$ fm) ensemble with $m_l = 0.2m_s$. However, the analysis presented below is restricted to full QCD data from the coarse $0.4m_s$ and $0.2m_s$ ensembles and the fine ensembles shown in Table 1.

Table 1: MILC ensembles [5, 6, 7] for the current round of $D \to \pi(K)l\nu$ analyses, together with the valence masses used for all ensembles at each lattice spacing. Valence masses after the semicolons are the tuned strange mass. Data generation is complete for all ensembles and quark masses shown.

	$\approx a$ (fm)	am_l/am_s	$N_s^3 \times N_t$	N_{conf}	am_{valence}
coarse	0.12	0.02/0.05	$20^3 \times 64$	2052	0.005, 0.007, 0.01,
		0.01/0.05	$20^3 \times 64$	2259	0.02, 0.03, 0.0415,
		0.007/0.05	$20^3 \times 64$	2110	0.05; 0.0349
		0.005/0.05	$24^3 \times 64$	2099	
fine	0.09	0.0124/0.031	$28^3 \times 96$	1996	0.0031, 0.0047, 0.0062,
		0.0062/0.031	$28^3 \times 96$	1946	0.0093, 0.0124, 0.031;
		0.0031/0.031	$40^3 \times 96$	1015	0.0261
superfine	0.06	0.0072/0.018	$48^3 \times 144$	593	0.0036, 0.0072, 0.0018,
		0.0036/0.018	$48^3 \times 144$	668	0.0025, 0.0054, 0.0160;
					0.0188

2.2 Correlators, correlator ratios, and ratio fits

To extract the matrix elements $\langle \pi | V_\mu | D \rangle$ corresponding to $f_{\parallel,\perp}^{D\pi}(q^2)$, we use ratios of 3-point to 2-point correlators designed to cancel oscillations of opposite-parity states in staggered correlators [8]. To minimize statistical errors and avoid excited-state contamination, we generate the 3-point correlators at two source-sink separations [9]. The structure of the 3-point correlators is shown in Fig. 1. The 3-point correlators are computed with current insertions at all times between the source and sink. For insertion times far from the source and sink, plateaus appear in the ratios. These plateaus are proportional to the desired form factors $f_\parallel^{D\pi}$ and $f_\perp^{D\pi}$.

We are studying combinations of fit ranges, fit functions, source-sink–separations, and momenta to minimize errors and control excited-state contamination. Fits to ratios yielding $f_\parallel^{D\pi}$ on the coarse $0.1m_s$ ensemble are shown in Fig. 2; we fit to a constant with an exponential on the D-side of the 3-point correlator to account for leading excited-state contributions; the resulting

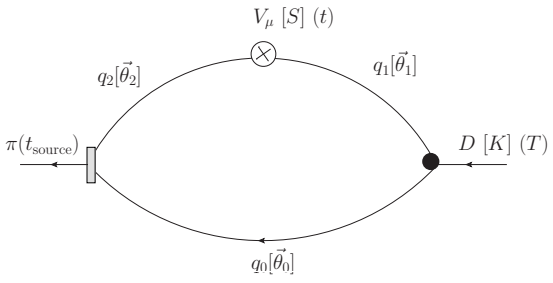

Figure 1: Structure of the 3-point functions needed to calculate $f_{\parallel,\perp}^{D\pi}[f_0^{K\pi}]$. Light quark propagators are generated at t_{source} with local sources [random wall sources]. An extended charm [strange] propagator is generated at T.

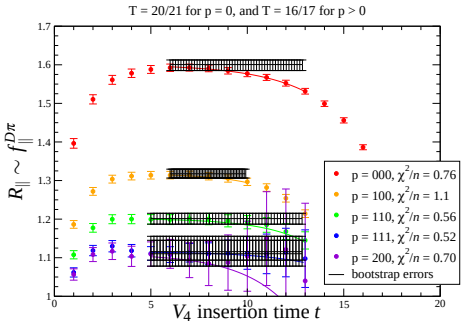

Figure 2: Fits of preliminary results for $f_\parallel^{D\pi}$ to plateaus and excited-state exponentials. Errors are statistical only and were obtained from 500 bootstrap ensembles.

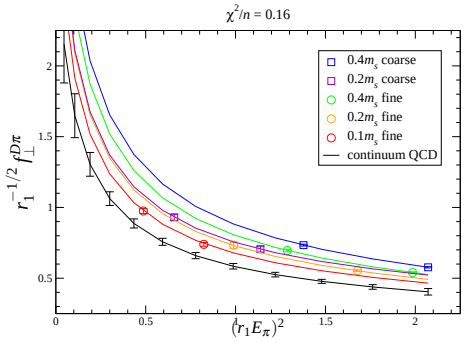

Figure 3: A simultaneous fit to SχPT of all $f_\perp^{D\pi}$ data from the indicated ensembles. Errors are statistical and were obtained with 500 bootstrap ensembles. The black curve is the continuum result at physical quark masses and fiducial energies.

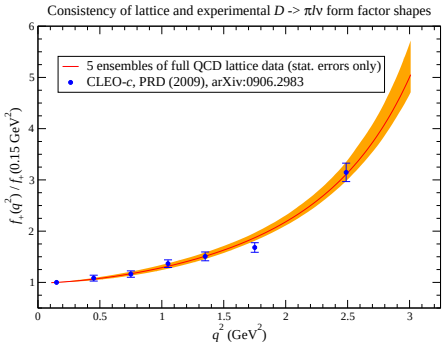

Figure 4: Overlay of the ratio $f_+^{D\pi}(q^2)/f_+^{D\pi}(\tilde{q}^2)$ from the lattice (red curve and orange error band) and CLEO (blue points). The orange error band shows statistical lattice errors, and the blue error bars, the full experimental errors. At $\tilde{q}^2 = 0.15$ GeV^2, the results agree and the errors vanish by definition.

curves are consistent with the data. In Fig. 2 we also plot the resulting plateau terms and bootstrap errors over the entire fit ranges. Consistent with expectations [9], we find the larger source-sink separation is optimal for $\mathbf{p} = \mathbf{0}$, while the smaller source-sink separation is optimal for $|\mathbf{p}| > 0$.

2.3 Renormalization and blinding

We need to renormalize the current. This provides an easy way to do a blind analysis. After nonperturbatively renormalizing the quark fields in the current, the remaining lattice artifacts at leading order in HQET are perturbatively calculable. A subset of our collaboration is calculating this correction, which enters the result as an overall multiplicative factor depending on the ensemble and valence masses. By including an offset in this factor, the normalization of the form factors and the implied value of $|V_{cd}|$ is masked from analysts performing fits, thereby eliminating a potential source of bias.

2.4 Chiral-continuum-energy extra-interpolation

We fit the form factors $f_{\parallel,\perp}^{D\pi}$ obtained from the correlator ratios to NLO heavy-meson SχPT [10] and extrapolate the results to the physical quark masses and continuum limit. For the comparison below of lattice and experimental results, we also used SχPT to describe the energy dependence of the form factor, and we supplement the NLO expressions with NNLO terms analytic in the quark masses and lattice spacing. Although we include data from only a subset of the ensembles (cf. Sec. 2.1), we perform a simultaneous fit to all data from all ensembles included. We include momenta through $\frac{2\pi}{aN_s}(1,1,0)$ and obtain statistical errors by propagating the bootstrap errors from the ratio fits. A fit to the data for $f_\perp^{D\pi}$ is shown in Fig. 3. The results are stable under variations of the prior central values and addition of NNNLO analytic terms.

2.5 Comparison of lattice and experimental form factor shapes

To compare our result with experiment, we consider the ratio $f_+^{D\pi}(q^2)/f_+^{D\pi}(\tilde{q}^2)$, where $\tilde{q}^2 \equiv 0.15$ GeV^2 is a convenient but otherwise arbitrary reference point. The ratio $f_+^{D\pi}(q^2)/f_+^{D\pi}(\tilde{q}^2)$ can

be fixed from experiment without the CKM matrix element $|V_{cd}|$. Using this ratio to compare the shapes of the lattice and experimental results also cancels the blinding factor. The use of this type of ratio to compare lattice and experimental results was advocated in [11].

In Fig. 4, we overlay the (preliminary) lattice and (currently final) experimental results for the ratio $f_+^{D\pi}(q^2)/f_+^{D\pi}(\tilde{q}^2)$. The red curve shows the lattice central value, and the orange error band shows the bootstrap errors. The blue data points show the experimental central values, and the blue error bars, the statistical and systematic errors from the full covariance matrix [3].

2.6 $D \to \pi l \nu$: Summary and next steps

The shape of our preliminary result for the $D \to \pi l \nu$ form factor, obtained from a subset of our data, closely matches the shape seen in the CLEO data. This agreement encourages us to apply our methods to the calculations of the B semileptonic form factors and related searches for new physics. The statistical errors in the lattice form factor at the fiducial value $\tilde{q}^2$ are about 5%, in accord with expectations [9]. We are adding to the analysis partially quenched and full QCD data from the remaining two coarse ensembles in Table 1 and the superfine $0.4m_s$ and $0.2m_s$ ensembles. Estimates of heavy quark errors, the uncertainty propagated from the $D^*D\pi$ coupling, and other systematics are in progress.

Finally, we are exploring combining information about the energy-dependence of the form factors from the z-expansion with information about the quark mass and lattice spacing dependence from SχPT by using SχPT to compute the mass and lattice spacing dependence of the Taylor coefficients in the z-expansion. This approach furnishes an alternative to SχPT for model-independent, simultaneous fits of data at all energies on all ensembles, and is similar to, but distinct from, that detailed in [12].

3. $K \to \pi l \nu$: Exploring methodology to simulate at $q^2 = 0$

One of the most significant systematic errors in traditional lattice analyses of $K \to \pi l \nu$ arises because correlation functions with periodic boundary conditions do not cover the physical region of q^2, so obtaining $f_+^{K\pi}(q^2 = 0)$ and extracting $|V_{us}|$ from experimental data requires interpolating between q^2_{max} and unphysical values of q^2. Model dependence is introduced by the choice of interpolating function. We want to eliminate this systematic error by using twisted boundary conditions to simulate at $q^2 \simeq 0$. This approach was first suggested in [13] and later exploited with 2+1 flavors of domain wall fermions in [14] and 2 flavors of twisted mass fermions in [15].

The other main component of our analysis is the method developed by the HPQCD Collaboration to study D semileptonic decays [16]. This method is based on the Ward identity relating the matrix element of a vector current to that of the corresponding scalar current $q^\mu \langle \pi | V_\mu^{lat.} | K \rangle Z = (m_s - m_q) \langle \pi | S^{lat.} | K \rangle$, with $S = \bar{s}l$, and Z, a lattice renormalization factor for the vector current. Using the definition of the form factors in Eq. (1.1) and this identity, one can extract $f_0^{K\pi}(q^2)$ at any q^2 by using

$$f_0^{K\pi}(q^2) = \frac{m_s - m_l}{m_K^2 - m_\pi^2} \langle \pi | S | K \rangle (q^2). \tag{3.1}$$

The kinematic constraint requires $f_+(0) = f_0(0)$, so this relation can be used to calculate $f_+^{K\pi}(0)$. The downside of the method is that it gives no access to the shape of $f_+^{K\pi}$, but that is very well known from experiment [4]. For more details of this method, see [16].

3.1 Test run: simulation and fitting details

The main goal of this test run is a realistic estimate of the statistical errors we could achieve and an assessment of how easily we can tune the twisting angles to get values of q^2 close to zero. For these tests we used about 500–600 configurations from each of the coarse $0.2m_s$ and $0.4m_s$ ensembles, and ~ 550 configurations for the fine $0.2m_s$ ensemble. Instead of using the asqtad action for the light and strange valence quarks, as in our calculation of the $D \to \pi l \nu$ form factor, we use the HISQ formulation [17], which has better control of discretization effects.

We generate 3-point correlators as shown in Fig. 1 with a scalar insertion at time t and 2-point functions for kaons and pions using both local and random wall sources. The latter sources produce results with statistical errors 2–3 times smaller than the former, so in the following discussion we consider only the results obtained with random wall sources. We inject momentum in the 2-point functions by using twisted boundary conditions to generate (one of) the light propagators. For the 3-point functions, we inject the momentum $\mathbf{p} = \boldsymbol{\theta}\pi/L$ in either the kaon or the pion by choosing either $\boldsymbol{\theta}_0 = \boldsymbol{\theta}_2 = \mathbf{0}$, $\boldsymbol{\theta}_1 \neq \mathbf{0}$ or $\boldsymbol{\theta}_0 = \boldsymbol{\theta}_1 = \mathbf{0}$, $\boldsymbol{\theta}_2 \neq \mathbf{0}$, respectively (see Fig. 1). The different external momenta and resulting q^2 are shown in Table 2. We have obtained two values of q^2 very close to zero by tuning the twisting angle from 2-point correlator fits only. To extract the form factor, we fit the 3-point and 2-point correlators together, which gives us slightly different values for q^2, but still close enough to zero to avoid any significant interpolation in q^2. In fact, the values of $f_+^{K\pi}(q^2 \simeq 0)$ that we obtain from the correlators with external momentum injected in the kaon and the pion agree within one sigma.

We repeat the combined fits using iterative averages of the correlators at different values of t and T to suppress oscillations due to opposite-parity states [8], including the ground state and first oscillating contributions. We use fits to the ground state alone and fits including four exponentials to crosscheck the central values and errors.

$\lvert\boldsymbol{\theta}_1\rvert$	$\lvert\boldsymbol{\theta}_2\rvert$	$(r_1 q)^2$
0	0	0.0227(3)
0	**0.7295**	**0.0011(4)**
0.7295	0	0.0153(3)
0	0.9105	-0.0109(5)
0.9105	0	0.0114(5)
1.2876	**0**	**0.0003(3)**

Table 2: Simulation values of the twisting angles $\boldsymbol{\theta}_1$ and $\boldsymbol{\theta}_2$, and the corresponding q^2. Errors are statistical. The smallest q^2 available with periodic boundary conditions is $\simeq -0.104$, already outside the physical region. Lines in bold correspond to $q^2 \simeq 0$.

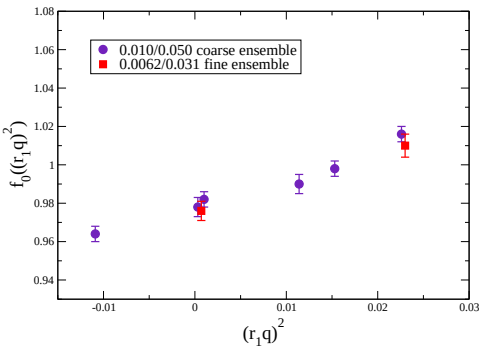

Figure 5: Form factor $f_0^{K\pi}$ as a function of momentum transfer q^2 for the coarse and fine lattice points.

3.2 Test results and future plans

The results for the $f_0^{K\pi}(q^2)$ form factor for the different values of q^2 simulated on the $0.2m_s$ coarse and fine lattices are shown in Fig. 5. The statistical errors for the two coarse points and the fine point with $q^2 \simeq 0$ are about 0.4%. In Fig. 5 one can see that the form factors for $a \simeq 0.12, 0.09\,\text{fm}$ agree with each other within statistics, suggesting very small discretization effects. Similar behavior is observed when comparing results with $m_l = 0.2m_s$ and $m_l = 0.4m_s$ on the coarse lattices. Such behavior suggests that, after extrapolation to the continuum and the physical sea light quark masses, residual effects for those error sources will be negligible.

Using the full statistics available in these ensembles, around 4 times the number of configurations used here, we expect statistical errors around $0.2-0.3\%$. Since we will eliminate the uncertainty due to the q^2 interpolation by simulating at $q^2 \simeq 0$, the only significant remaining error besides statistics will be the one associated with the chiral-continuum extrapolation. We plan to do this extrapolation using continuum χPT at NNLO and incorporate taste-breaking effects at NLO, including data from at least three different lattice spacings and light quark masses down to $m_s/8$. Based on the tests described here, we expect our calculation to be competitive with the existing state-of-the-art calculations of $f_+^{K\pi}(0)$ [14, 15].

References

[1] A review is R. S. Van de Water, PoS **LAT2009**, 014 (2009) [arXiv:0911.3127 [hep-lat]].

[2] A. X. El-Khadra, A. S. Kronfeld, P. B. Mackenzie, S. M. Ryan and J. N. Simone, Phys. Rev. D **64** (2001) 014502 [arXiv:hep-ph/0101023].

[3] D. Besson *et al.* [CLEO], Phys. Rev. D **80**, 032005 (2009) [arXiv:0906.2983 [hep-ex]].

[4] For a review of current results see, for example, M. Antonelli *et al.*, Phys. Rept. **494** (2010) 197 [arXiv:0907.5386 [hep-ph]].

[5] A. Bazavov *et al.*, Rev. Mod. Phys. **82** (2010) 1349 [arXiv:0903.3598 [hep-lat]].

[6] C. W. Bernard *et al.* [MILC], Phys. Rev. D **64**, 054506 (2001) [arXiv:hep-lat/0104002].

[7] C. Aubin *et al.* [MILC], Phys. Rev. D **70**, 094505 (2004) [arXiv:hep-lat/0402030].

[8] J. A. Bailey *et al.*, Phys. Rev. D **79**, 054507 (2009) [arXiv:0811.3640 [hep-lat]].

[9] J. A. Bailey *et al.* [Fermilab Lattice, MILC], PoS **LAT2009**, 250 (2009) [arXiv:0912.0214 [hep-lat]].

[10] C. Aubin and C. Bernard, Phys. Rev. D **76**, 014002 (2007) [arXiv:0704.0795 [hep-lat]].

[11] C. Bernard *et al.*, Phys. Rev. D **80** (2009) 034026 [arXiv:0906.2498 [hep-lat]].

[12] H. Na, C. T. H. Davies, E. Follana *et al.*, [arXiv:1008.4562 [hep-lat]].

[13] J. M. Flynn, A. Jüttner and C. T. Sachrajda [UKQCD Collaboration], Phys. Lett. B **632** (2006) 313 [arXiv:hep-lat/0506016].

[14] P. A. Boyle *et al.*, arXiv:1004.0886 [hep-lat].

[15] V. Lubicz *et al.*, Phys. Rev. D **80** (2009) 111502 [arXiv:0906.4728 [hep-lat]].

[16] H. Na *et al.*, PoS **LAT2009**, 247 (2009) [arXiv:0910.3919 [hep-lat]]; [arXiv:1008.4562 [hep-lat]].

[17] E. Follana *et al.* [HPQCD, UKQCD], Phys. Rev. D **75** (2007) 054502 [arXiv:hep-lat/0610092].